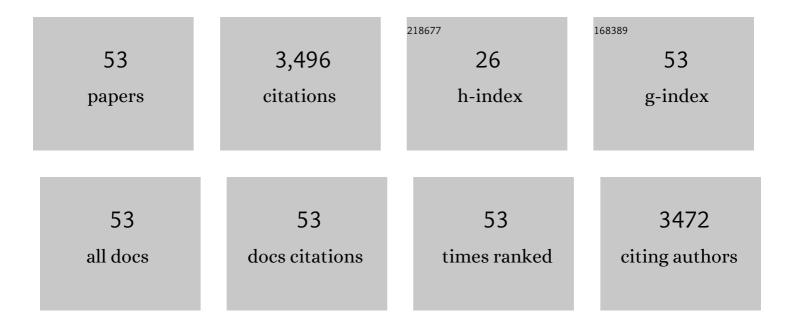
## Ying Wang

List of Publications by Year in descending order

Source: https://exaly.com/author-pdf/4131893/publications.pdf Version: 2024-02-01



YING WANG

#	Article	IF	CITATIONS
1	Zn-vacancy mediated electron-hole separation in ZnS/g-C3N4 heterojunction for efficient visible-light photocatalytic hydrogen production. Applied Catalysis B: Environmental, 2018, 229, 41-51.	20.2	529
2	Band Structure Engineering of Carbon Nitride: In Search of a Polymer Photocatalyst with High Photooxidation Property. ACS Catalysis, 2013, 3, 912-919.	11.2	450
3	Zinc vacancy-promoted photocatalytic activity and photostability of ZnS for efficient visible-light-driven hydrogen evolution. Applied Catalysis B: Environmental, 2018, 221, 302-311.	20.2	427
4	Enhanced photocarrier separation in conjugated polymer engineered CdS for direct Z-scheme photocatalytic hydrogen evolution. Applied Catalysis B: Environmental, 2020, 260, 118131.	20.2	200
5	Architecture of high efficient zinc vacancy mediated Z-scheme photocatalyst from metal-organic frameworks. Nano Energy, 2018, 52, 105-116.	16.0	179
6	Facile green synthesis of crystalline polyimide photocatalyst for hydrogen generation from water. Journal of Materials Chemistry, 2012, 22, 15519.	6.7	134
7	Developing a polymeric semiconductor photocatalyst with visible light response. Chemical Communications, 2010, 46, 7325.	4.1	132
8	Sulfur-Doped Polyimide Photocatalyst with Enhanced Photocatalytic Activity under Visible Light Irradiation. ACS Applied Materials & Interfaces, 2014, 6, 4321-4328.	8.0	103
9	Melem: A metal-free unit for photocatalytic hydrogen evolution. International Journal of Hydrogen Energy, 2014, 39, 13519-13526.	7.1	98
10	Constructing a High-Efficiency MoO <sub>3</sub> /Polyimide Hybrid Photocatalyst Based on Strong Interfacial Interaction. ACS Applied Materials & Interfaces, 2015, 7, 14628-14637.	8.0	97
11	Self-constructed facet junctions on hexagonal CdS single crystals with high photoactivity and photostability for water splitting. Applied Catalysis B: Environmental, 2019, 244, 694-703.	20.2	93
12	Bandgap modulation of polyimide photocatalyst for optimum H2 production activity under visible light irradiation. International Journal of Hydrogen Energy, 2013, 38, 10768-10772.	7.1	78
13	Confinement effect of monolayer MoS <sub>2</sub> quantum dots on conjugated polyimide and promotion of solar-driven photocatalytic hydrogen generation. Dalton Transactions, 2017, 46, 3877-3886.	3.3	72
14	Fabrication of a new MgO/C sorbent for CO2 capture at elevated temperature. Journal of Materials Chemistry A, 2013, 1, 12919.	10.3	61
15	In situ growth MoO3 nanoflake on conjugated polymer: An advanced photocatalyst for hydrogen evolution from water solution under solar light. Solar Energy Materials and Solar Cells, 2016, 150, 102-111.	6.2	53
16	TiO <sub>2</sub> as an interfacial-charge-transfer-bridge to construct eosin Y-mediated direct Z-scheme electron transfer over a Co <sub>9</sub> S <sub>8</sub> quantum dot/TiO <sub>2</sub> photocatalyst. Catalysis Science and Technology, 2020, 10, 5267-5280.	4.1	48
17	A (001) dominated conjugated polymer with high-performance of hydrogen evolution under solar light irradiation. Chemical Communications, 2017, 53, 10536-10539.	4.1	47
18	Fabricating direct Z-scheme PTCDA/g-C3N4 photocatalyst based on interfacial strong interaction for efficient photooxidation of benzylamine. Applied Surface Science, 2018, 456, 861-870.	6.1	45

YING WANG

#	Article	IF	CITATIONS
19	A novel porous MgO sorbent fabricated through carbon insertion. Journal of Materials Chemistry A, 2014, 2, 12014-12022.	10.3	41
20	Polyimide-based photocatalysts: rational design for energy and environmental applications. Journal of Materials Chemistry A, 2020, 8, 14441-14462.	10.3	38
21	Trapping the lead ion in multi-components aqueous solution by natural clinoptilolite. Journal of Hazardous Materials, 2010, 180, 282-288.	12.4	37
22	Molecule-induced gradient electronic potential distribution on a polymeric photocatalyst surface and improved photocatalytic performance. Journal of Materials Chemistry A, 2013, 1, 5142.	10.3	35
23	Constructing direct Z-scheme CuO/PI heterojunction for photocatalytic hydrogen evolution from water under solar driven. International Journal of Hydrogen Energy, 2021, 46, 9064-9076.	7.1	32
24	Ultrathin conjugated polymer nanosheets as highly efficient photocatalyst for visible light driven oxygen activation. Applied Catalysis B: Environmental, 2020, 277, 119228.	20.2	30
25	Liquid adsorption of tobacco specific N-nitrosamines by zeolite and activated carbon. Microporous and Mesoporous Materials, 2014, 200, 260-268.	4.4	28
26	Developing high-efficiency π conjugated polymer semiconductor for photocatalytic degradation of dyes under visible light irradiation. RSC Advances, 2014, 4, 57153-57158.	3.6	28
27	New Solid-Base Cu–MgO for CO <sub>2</sub> Capture at 473 K and Removal of Nitrosamine. ACS Applied Materials & Interfaces, 2016, 8, 30193-30204.	8.0	23
28	New activated carbon sorbent with the zeolite-like selectivity to capture tobacco-specific nitrosamines in solution. Chemical Engineering Journal, 2018, 339, 170-179.	12.7	23
29	Porphyrinâ€containing Polyimide with Enhanced Light Absorption and Photocatalysis Activity. Chemistry - an Asian Journal, 2019, 14, 2138-2148.	3.3	23
30	New efficient selective adsorbent of tobacco specific nitrosamines derived from discarded cigarette filters. Microporous and Mesoporous Materials, 2019, 284, 393-402.	4.4	23
31	Novel phenol capturer derived from the as-synthesized MCM-41. Journal of Hazardous Materials, 2011, 190, 87-93.	12.4	22
32	Trapping tobacco specific N-nitrosamines in Chinese-Virginia type tobacco extracting solution by porous material. Journal of Porous Materials, 2014, 21, 311-320.	2.6	22
33	Capturing tobacco specific N-nitrosamines (TSNA) in industrial tobacco extract solution by ZnO modified activated carbon. Microporous and Mesoporous Materials, 2016, 222, 160-168.	4.4	20
34	Creating an Optimal Microenvironment within Mesoporous Silica MCM-41 for Capture of Tobacco-Specific Nitrosamines in Solution. ACS Applied Materials & Interfaces, 2017, 9, 26805-26817.	8.0	19
35	Liquid adsorption and catalytic degradation of 4-methylnitrosamino-1-3-pyridyl-1-butanone (NNK) by zeolite. Microporous and Mesoporous Materials, 2017, 243, 39-46.	4.4	17
36	<i>In situ</i> growth of MOF-derived sulfur vacancy-rich CdS nanoparticles on 2D polymers for highly efficient photocatalytic hydrogen generation. Dalton Transactions, 2022, 51, 5841-5858.	3.3	17

YING WANG

#	Article	IF	CITATIONS
37	Creating the adsorptive sites with high performance toward nitrosamines in mesoporous silica MCM-41 by alumina modifier. Microporous and Mesoporous Materials, 2009, 126, 143-151.	4.4	16
38	Novel mesoporous composite with zeolite-like selectivity to capture tobacco specific nitrosamine NNK. Chemical Engineering Journal, 2018, 332, 331-339.	12.7	16
39	New shape-selectivity discovered on graphene-based materials in catching tobacco specific nitrosamines. Journal of Hazardous Materials, 2018, 358, 234-242.	12.4	16
40	Efficiently capturing tobacco specific nitrosamines with Hβ zeolite in solution. Journal of Hazardous Materials, 2019, 365, 196-204.	12.4	16
41	New sucker-type precise capturer of tobacco specific nitrosamines derived from the SBA-15 in situ modified with polyaniline. Chemical Engineering Journal, 2018, 354, 1174-1184.	12.7	15
42	Impact of proton: Capturing tobacco specific N -nitrosamines (TSNA) with HZSM-5 zeolite. Chemical Engineering Journal, 2017, 323, 180-190.	12.7	14
43	A new triazine-based conjugated polymer from simple monomers with stable photocatalytic hydrogen evolution under visible light. Polymer, 2020, 211, 123079.	3.8	12
44	Controllable Conformation Transfer of Conjugated Polymer toward High Photoelectrical Performance: The Role of Solvent in Induced-Crystallization Route. Journal of Physical Chemistry C, 2018, 122, 1037-1043.	3.1	10
45	Spatially separated cocatalysts for efficient charge separation: a hollow Pt/CdS/N–ZnO/CoOx graphene microtubule with high stability for photocatalytic reactions and sustainable recycling. Catalysis Science and Technology, 2019, 9, 6899-6908.	4.1	10
46	Fabricating hydrophobic nanoparticles within mesoporous channel of silica for efficient TSNA removal. Microporous and Mesoporous Materials, 2017, 237, 237-245.	4.4	9
47	Highly efficient hydrogen evolution from water splitting on heptazine polymer with three types of defects. Applied Surface Science, 2022, 580, 152070.	6.1	7
48	Insight into the liquid adsorption of tobacco specific nitrosamines on ZIF-8. Microporous and Mesoporous Materials, 2022, 333, 111730.	4.4	7
49	New versatile zincic sorbent for tobacco specific nitrosamines and lead ion capture. Journal of Hazardous Materials, 2020, 383, 121188.	12.4	6
50	Solvothermal synthesis of porous conjugated polymer with high surface area for efficient adsorption of organic and biomolecules. Journal of Porous Materials, 2018, 25, 1659-1668.	2.6	5
51	Sustainable sorbent derived from discarded cigarette butts for elimination of tobacco specific nitrosamines carcinogen. Environmental Technology and Innovation, 2021, 24, 101825.	6.1	5
52	Insight into the efficient TSNA capturer derived from zeolite Hβ. Chemical Engineering Journal, 2019, 369, 480-488.	12.7	4
53	New environmental selective micro-mesoporous carbonaceous sorbent for eliminating tobacco specific nitrosamines and lead ion. Microporous and Mesoporous Materials, 2021, 318, 111037.	4.4	4